Structure in Solution of M1 RNA, the Catalytic Subunit of Ribonuclease P from *Escherichia coli*†

Cecilia Guerrier-Takada and Sidney Altman*

ABSTRACT: The structure of M1 RNA, the RNA component of *Escherichia coli* RNase P, has been probed by mild digestion with a variety of ribonucleases. The results have been used to generate a model for the two-dimensional structure of M1 RNA. This model is similar in many respects to an earlier model that was based entirely on theoretical considerations. M1 RNA was digested with RNase T_1 in buffer containing 10 mM $MgCl_2$ (in which M1 RNA, by itself, has no catalytic activity) and in buffer containing 60 mM $MgCl_2$ (in which M1 RNA can cleave precursors to tRNA molecules). Under these conditions, the main features of the secondary structure are similar, but several minor differences are apparent. Such subtle changes in structure are also observed when M1 RNA is present in a binary complex with a substrate molecule, the precursor to *E. coli* $tRNA^{Tyr}$.

We have recently shown that M1 RNA[1] is the catalytic subunit of RNase P and that it alone governs the binding of the tRNA substrates to the holoenzyme (Altman et al., 1980; Guerrier-Takada et al., 1983; Guerrier-Takada & Altman, 1984). We have now undertaken a detailed examination of the structure of M1 RNA in order to determine how it performs its catalytic function and how it interacts with the protein cofactor which is essential for the activity of RNase P in vivo. Complementation experiments in vitro using subunits of RNase P purified from *Escherichia coli* and *Bacillus subtilis* indicate that the structure in solution of the RNA subunit plays an important role in the function of RNase P. We have examined the secondary structure of *E. coli* M1 RNA by using ribonucleases which have been previously used in studies of the structure of nucleic acids in solution. Controlled cleavages were performed by using ribonucleases A and T_1 and nuclease S_1, which have preference for cleavage in single-stranded regions of RNA, and *Naja naja oxiana* cobra venom ribonuclease, which cleaves RNA within double-stranded regions (Avron et al., 1982; Garret & Olesen, 1982; Wurst et al., 1978; Vasilenko et al., 1983). In addition, using RNase T_1, which yields reproducible patterns of digestion within a wide range of Mg ion concentration, we have compared the susceptibility of M1 RNA to nuclease digestion in buffers containing 60 mM $MgCl_2$ (catalytically active form) and 10 mM $MgCl_2$ (inactive form) and that of reconstituted RNase P (M1 RNA plus C5 protein) in buffer containing 10 mM $MgCl_2$ (active form). Such studies were also carried out with a binary complex (M1 RNA plus substrate pTyr)[2] and a ternary complex (M1 RNA plus C5 protein plus pTyr). Several subtle differences in M1 RNA structure were observed between the active (with and without substrate) and inactive forms, but the main features of secondary structure were preserved.

Materials and Methods

Enzymes and Reagents. Ribonucleases T_1 and A were purchased from Calbiochem. Nuclease S_1 and alkaline phosphatase from calf intestine were obtained from Boehringer-Mannheim. T4 RNA ligase was obtained from P-L Biochemicals. T4 polynucleotide kinase was purchased from Bethesda Research Laboratories. Radioactive nucleotides were obtained from Amersham Radiochemicals and New England Nuclear Corp. All other chemicals were reagent grade. Cobra venom nuclease was a generous gift of Dr. J. Vournakis (Syracuse University).

Preparation of Unlabeled and Uniformly Labeled M1 RNA. M1 RNA was prepared as described by Reed et al. (1982).

3′ End Labeling of M1 RNA. M1 RNA molecules were labeled at their 3′ termini with T4 RNA ligase and [5′-^{32}P]pCp under conditions similar to those described by England et al. (1980). The reaction was carried out in 30 μL of 50 mM Hepes, pH 7.5, 20 mM $MgCl_2$, 3.3 mM DTT, 10% Me_2SO, and 300 ng of bovine serum albumin and contained 20 pmol of M1 RNA, 40 pmol of [5′-^{32}P]pCp, 180 pmol of ATP, and 5 units of T4 RNA ligase. The reaction mixture was incubated overnight (12–15 h) at 4 °C and the reaction terminated by the addition of 5 μL of liquefied phenol to inactivate the enzyme. Carrier tRNA ($0.5OD_{260}$) and salt (0.25 M NaOAc) were added, and the RNA was precipitated with ethanol. After two washes with 75% ethanol, the RNA pellet was lyophilized, resuspended in 50 μL of 10 M urea, 0.05% XC, and 0.05% BPB, and electrophoresed on a 20 × 40 × 0.15 cm polyacrylamide gel [5% acrylamide, 0.17% bis(acrylamide), 7 M urea, 50 mM Tris–borate, pH 8.3, and 1 mM EDTA]. A band corresponding to M1 RNA was visualized by autoradiography, excised from the gel, electroeluted from the gel slice, and used in partial nuclease digestion experiments and reconstitution assays for RNase P activity.

5′ End Labeling of M1 RNA. Unlabeled M1 RNA (36 μg) was dissolved in 100 μl of 50 mM Tris-HCl, pH 8.0, and 0.1 mM EDTA and incubated for 30 min at 37 °C with calf intestine alkaline phosphatase. The reaction mixture was extracted once with an equal volume of phenol, once with a

† From the Department of Biology, Yale University, New Haven, Connecticut 06520. *Received April 26, 1984.* This work was supported by U.S. Public Health Service Grant GM 19422 and National Science Foundation Grant PCM 8120788.

[1] Mature M1 RNA was originally reported to have 375 nucleotides (Reed et al., 1982). Recently, Sakamoto et al. (1983) have cloned the gene for M1 RNA from a different strain of *E. coli* from that originally used and have determined that the corresponding M1 RNA sequence has 377 nucleotides. On reexamination of a region of compression in nucleotide sequencing gels, we (R. Reed, personal communication) have confirmed the result of Sakamoto et al. (1983). The two additional nucleotides are $A_{195}G_{196}$ as shown in Figure 2.

[2] Abbreviations: pTyr, precursor to $tRNA^{Tyr}$ from *E. coli*; Hepes, *N*-(2-hydroxyethyl)piperazine-*N*′-2-ethanesulfonic acid; DTT, dithiothreitol; Me_2SO, dimethyl sulfoxide; Tris, tris(hydroxymethyl)aminomethane; EDTA, ethylenediaminetetraacetic acid; XC, xylene cyanol; BPB, bromphenol blue.

0006-2960/84/0423-6327$01.50/0

phenol–chloroform–isoamyl alcohol (1:0.96:0.04) mixture, and twice with chloroform (Maniatis et al., 1982). The RNA was precipitated with ethanol and the pellet washed twice with 75% ethanol. For 5′ end labeling, 3–6 μg of dephosphorylated M1 RNA was incubated at 37 °C for 30 min with 20 pmol of [γ-^{32}P]ATP in 30 μL of 70 mM Tris-HCl, pH 7.6, 10 mM $MgCl_2$, 100 mM KCl, 5 mM DTT, and 6 units of T4 polynucleotide kinase. At the end of the incubation period, the reaction mixture was extracted as indicated above in the procedure for 3′ end labeling of M1 RNA.

Partial Nuclease Digestion of M1 RNA. Partial nuclease digestions of M1 RNA were performed as follows: all digestion mixtures (25–30 μL final volume) contained about (2–5) × 10^4 cpm of 3′ and 5′ end-labeled M1 RNA. After incubation, the ribonucleases were inactivated by addition of 5 μL of liquefied phenol. RNA fragments were precipitated with ethanol in the presence of carrier tRNA. After two washes with 75% ethanol, the samples were resuspended in 10 M urea, 0.05% BPB, and 0.05% XC and analyzed on 5% and 12% polyacrylamide sequencing gels.

Digests with RNases A and T_1 were carried out on terminally labeled M1 RNA dissolved in 25 μL of 4B buffer [50 mM Tris-HCl, pH 7.5, 10 mM $Mg(OAc)_2$, 500 mM NH_4Cl, and 6 mM 2-mercaptoethanol]. One microliter of a 50 units/mL solution of RNase T_1 or 1 μL of a 50 μg/mL solution of RNase A in TE buffer (10 mM Tris-HCl, pH 7.5, and 1 mM EDTA) was added to the solution containing M1 RNA which was then kept on ice for 1 min.

Further analyses of the partial digests of uniformly labeled M1 RNA with RNase T_1 were performed as described previously (Reed et al., 1982). After electrophoresis on 5% polyacrylamide–7 M urea gels (20 × 40 × 0.15 cm) made in 50 mM TEB buffer (50 mM Tris–borate, pH 8.3, and 1 mM EDTA), several RNA fragments were cut out of each gel and electroeluted. These fragments were subjected to a complete RNase digestion (M1 RNA was incubated with 5 μL of a 5000 units/mL solution of RNase T_1 in TE buffer for 30 min at 37 °C) and fingerprinted (Platt & Yanofsky, 1975).

Digests with nuclease S_1 were carried out on M1 RNA resuspended in 25 μL of S_1 buffer (30 mM NaOAc, pH 4.5, 300 mM NaCl, and 3 mM $ZnSO_4$). A total of 2000 units of S_1 nuclease were added, and the reaction mixture was incubated for 10 min at room temperature.

Digests with cobra venom (CV) nuclease were carried out on M1 RNA resuspended in 25 μL of CV buffer (10 mM Tris-HCl, pH 7.5, 2 mM $MgCl_2$, and 200 mM NaCl). The RNA was digested with 0.01 μL of CV nuclease for 5 min at 37 °C.

Mild alkaline hydrolysis of M1 RNA was carried out by using the conditions described by Donis-Keller et al. (1977). The hydrolysis fragments were used as molecular weight markers in the analysis by gel electrophoresis of the products of the partial digestion of M1 RNA.

Results

Nuclease Digestion of M1 RNA. Single-stranded regions of M1 RNA were probed by using three different nucleases: RNase T_1, which cleaves after G residues in non-base-paired regions under conditions of mild digestion; RNase A, which cleaves after pyrimidines in non-base-paired regions under conditions of mild digestion; and nuclease S_1, which cleaves after any residue in non-base-paired regions. RNase T_1 and RNase A were used first in buffers containing 10 mM Mg^{2+} in an effort to preserve the secondary and tertiary structure of M1 RNA which may be physiologically relevant. Nuclease S_1 enzyme is active only in buffers containing Zn^{2+}. Although some inconsistencies might be anticipated in the results obtained with the three enzymes because of the different divalent metal ions used in the various experiments, in reality this has not proved to be a serious problem.

Double-stranded regions of M1 RNA were probed with cobra venom nuclease which, like nuclease S_1, does not cleave between specific bases but is active only in base-paired regions. Reactions with this enzyme were carried out in buffers containing 2 mM Mg^{2+}.

M1 RNA molecules, labeled at either their 5′ or their 3′ termini, were digested with the various nucleases under conditions which, as much as possible, maintain the native structure of the RNA. Cleavage sites in the RNA were then located by denaturing the digested samples and separating the fragments by electrophoresis in sequencing gels. Representative examples of the results of these experiments are shown in Figure 1. In Figure 1A, note the comparisons between lanes 2 and 3, which show, respectively, the products of digestion with RNase T_1 and cobra venom nuclease. Very few, if any, of the cleavage products generated by the cleavages by one of these ribonucleases of 3′ end-labeled M1 RNA have the same mobility as those generated by cleavage with the other ribonuclease. As expected, each of these nucleases cleaves in different regions of M1 RNA according to the specificity of the nuclease. (Note that the left-hand set of lanes has identical samples with the mirror-image right-hand set; the right-hand set was layered on the gel before the left-hand set to allow resolution of larger fragments of M1 RNA. Note also the presence of some spontaneous breakdown products of M1 RNA in lane 1 which are also present as background fragments in the other lanes.) When digestion of M1 RNA with RNase T_1 is carried out in buffer containing 0.5 M NH_4Cl (the buffer, 4B, in which M1 RNA is stored without loss of activity for extended periods; see Materials and Methods), the pattern of fragments produced is the same whether or not free magnesium ion is present in the buffer (see Figure 1A, lanes 2 and 5).

Figure 1B illustrates the cleavage products generated from digestion of 5′ end-labeled M1 RNA with nuclease S_1, RNAse T_1, and cobra venom nuclease. Note again that the presumed specificity of these nucleases is accurately reflected in the observed distribution of the products of cleavage. The data shown in Figure 1 and similar data, resulting from digestion of M1 RNA with RNase A, were used to construct the model for the two-dimensional structure of M1 RNA which is shown in Figure 2. Not all cleavage sites observed in the partial nuclease digestion experiments were used in construction of this model. That is, sites which were much less susceptible to nuclease cleavage than others (weak vs. strong sites) or which were not reproducibly cleaved were left out of the data set used to construct the model (for example, compare G95 in Figure 1B, a strong site, to G16, a weak site).

The model for the secondary structure of M1 RNA (Figure 2) takes into account both the data from the nuclease digestion experiments and the structural characteristics of an earlier, theoretical model which is reproduced in Figure 3. Figure 2A shows the cleavage sites obtained by using RNase T_1 and cobra venon nuclease, and Figure 2B shows the cleavage sites obtained by using nuclease S_1 and RNase A. Some of the sites indicated in Figure 2 as being susceptible to nuclease attack are also marked in Figure 1. We have not attempted to distinguish between relative susceptibilities of sites in the data we have included in constructing the model shown in Figure 2. As is evident in Figure 2, not every region of M1 RNA is a target for one of the nucleases we have used. We presume

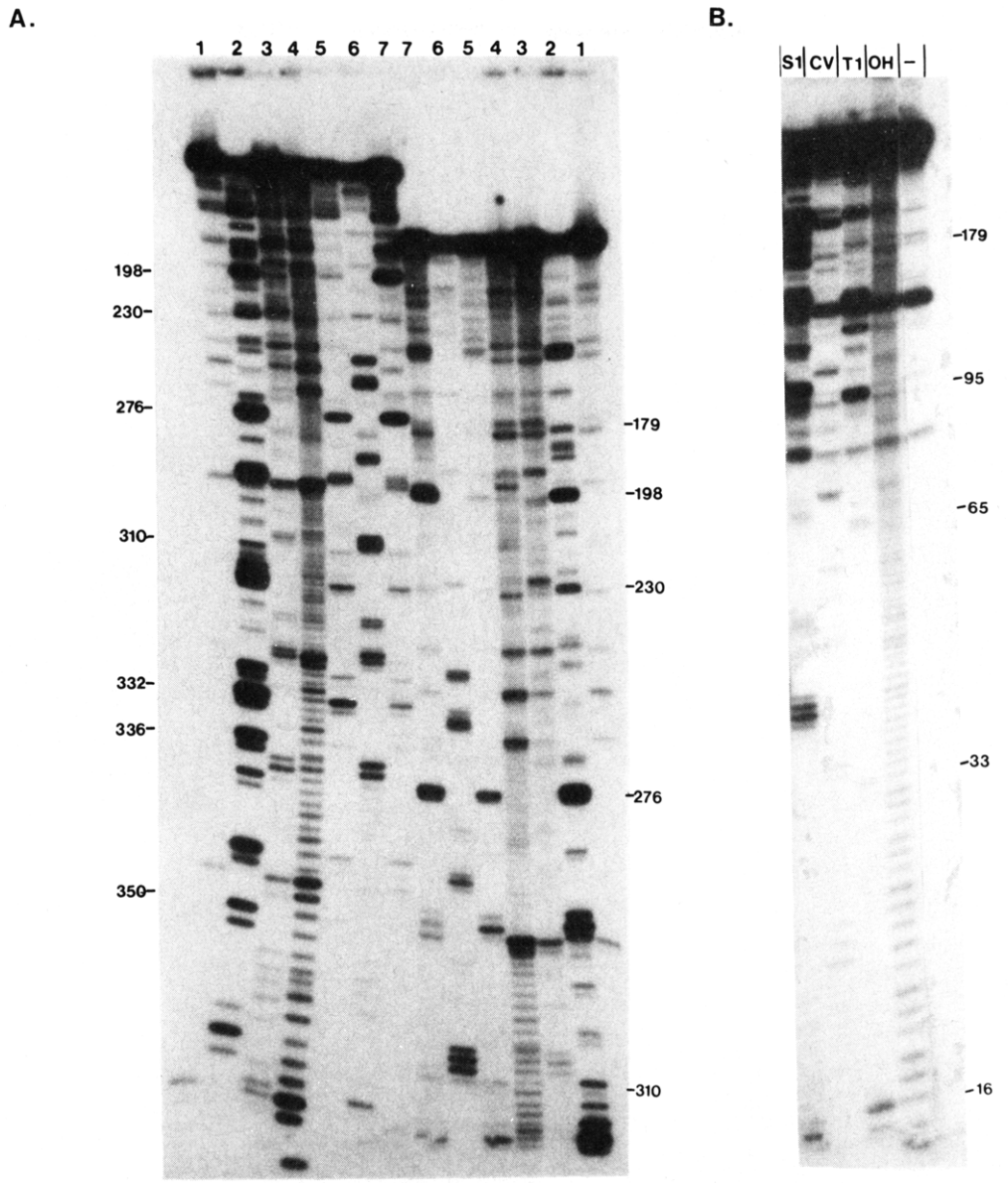

FIGURE 1: Autoradiograms of 3′ and 5′ end-labeled M1 RNA molecules electrophoresed on 12% polyacrylamide (sequencing) gels. Sites noted to be nuclease sensitive in several experiments are marked. As reported earlier (Reed et al., 1982), M1 RNA prepared from whole cell extracts has heterogeneous ends even after purification on several sequencing gels. Two major M1 RNA species which differ by one nucleotide in length at their 3′ termini are present in most preparations. This heterogeneity explains the apparent double cleavage sites obtained with RNase T_1 at positions 332 (and 333), 336 (and 337), etc. as shown in the figure. As the fragments from the partial nuclease digestion become larger in size (and appear closer to the origin of electrophoresis), the heterogeneity due to the extra nucleotide at the 3′ terminus is not longer apparent because of the limited resolution of the gel. (A) M1 RNA labeled at its 3′ terminus and treated as indicated. Buffers are described under Materials and Methods. Lane 1, no enzyme; lane 2, RNase T_1 (0 °C, 1 min) in 4B buffer lacking $MgCl_2$ but containing 10 mM EDTA; lane 3, cobra venom nuclease (37 °C, 5 min) in CV buffer; lane 4, mild alkaline digest; lane 5, RNase T_1 (0 °C, 1 min) in 4B buffer; lane 6, cobra venom nuclease (37 °C, 5 min) in 4B buffer; lane 7, nuclease S_1 (room temperature, 10 min). The seven samples on the left-hand side were identical with the right-hand set but were layered only after the bromphenol blue tracking dye in the right-hand set of samples was near the bottom of the gel. (B) M1 RNA labeled at its 5′ terminus and treated as indicated. Lane 1, nuclease S_1 (room temperature, 10 min); lane 2, cobra venom nuclease (37 °C, 5 min) in CV buffer; lane 3, RNase T_1 (0 °C, 1 min) in 4B buffer; lane 4, mild alkaline digest; lane 5, no enzyme.

these regions are occluded by tertiary structural interactions within M1 RNA. For this reason, there is still some uncertainty in the details of secondary structure in these regions. We have drawn the structures of these occluded regions to be compatible with the structure of adjacent parts of M1 RNA which are nuclease targets.

Features of the Model. The secondary structure of M1 RNA shown in Figure 2 has several interesting features. First, as with tRNAs and 5S RNA from *E. coli*, there is a base-paired stem structure formed between the nucleotides close to the 5′ and 3′ termini. Such stem structures involving the termini of RNAs may be necessary to protect these molecules from degradation by nonspecific exonucleases and may be a common feature of stable RNAs. We note that in M1 RNA there is some apparent susceptibility of the stem structure to cleavage near G–U base pairs and that the four 3′-termini nucleotides, though indicated as being unpaired, are susceptible to attack by cobra venom nuclease but not nuclease S_1. It is possible that these nucleotides are involved in tertiary structural interactions. For example, they are complementary to nucleotides 180–183 which are also susceptible to cobra venom nuclease and are shown in a loop structure in our model.

There are two pentanucleotide sequences in M1 RNA (331–335 and 284–288) which are complementary to the in-

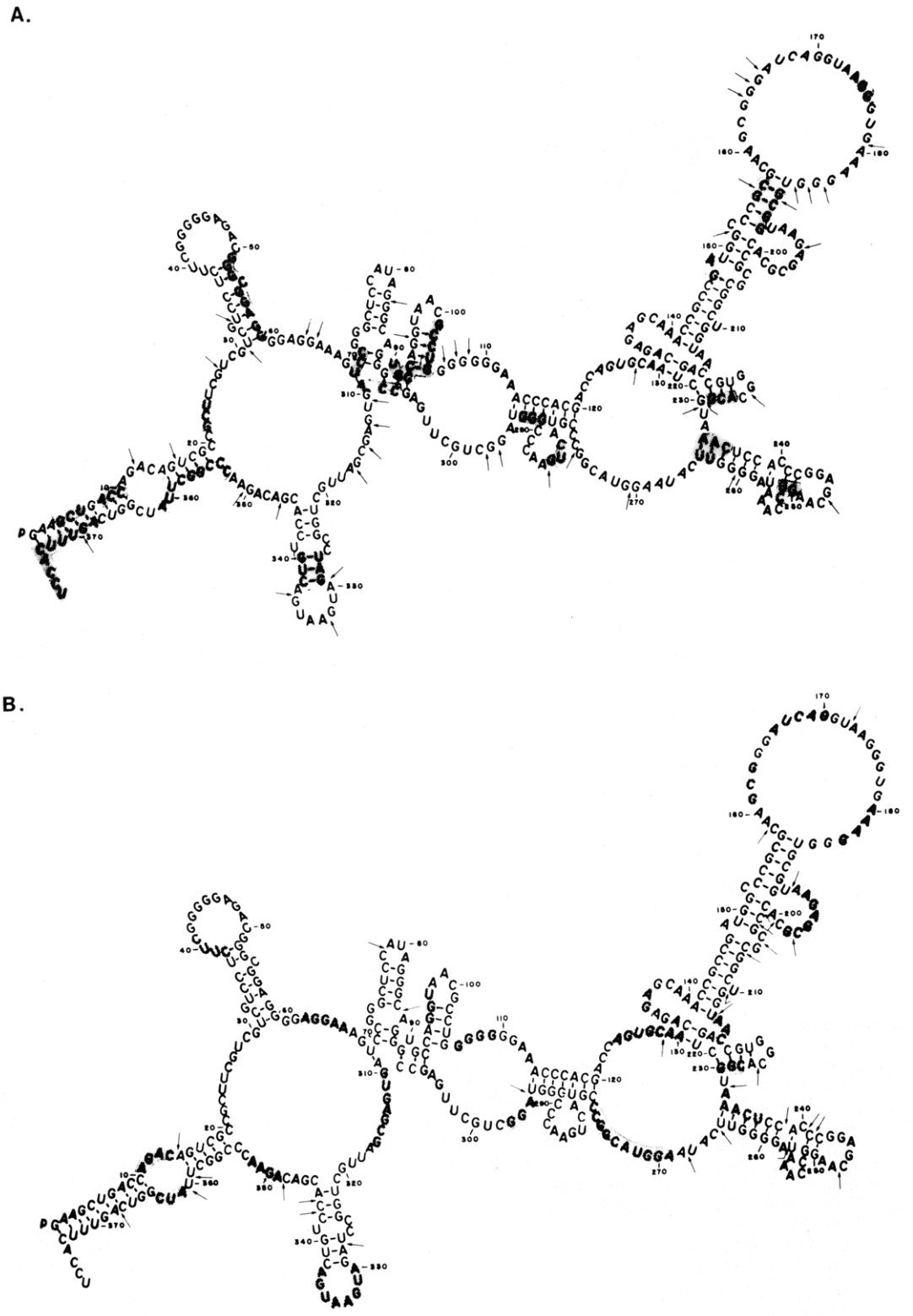

FIGURE 2: Model of the secondary structure of M1 RNA based on results of partial nuclease digestion experiments. (A) Sites of cleavage of M1 RNA by RNase T_1 (arrows) and by cobra venom nucleases (shaded areas). (B) Sites of cleavage of M1 RNA by nuclease S_1 (shaded areas) and RNase A (arrows).

variant GTΨCPu sequence found in all *E. coli* tRNAs. We proposed earlier that nucleotides 331–335 might be involved in substrate recognition by RNase P (Reed et al., 1982). Our data (Figure 2) show that these nucleotides are positioned in a loop structure and are available for hydrogen bonding with substrate molecules whereas nucleotides 284–288 are not readily cleaved by nucleases and are presumably buried in some folded region of M1 RNA, so that they are less accessible to pairing with other molecules. (Note that nucleotides 283–285 are susceptible to cobra venom nuclease but are placed in a loop structure. These nucleotides may be involved in a tertiary interaction responsible for folding of M1 RNA and which may also account for the inaccessibility to nucleases of adjacent nucleotides.)

The role of nucleotides 331–335 in substrate recognition that we originally proposed must, however, be brought into question since M. Baer has shown (personal communication) that changing nucleotide 333 from A to C does not alter the

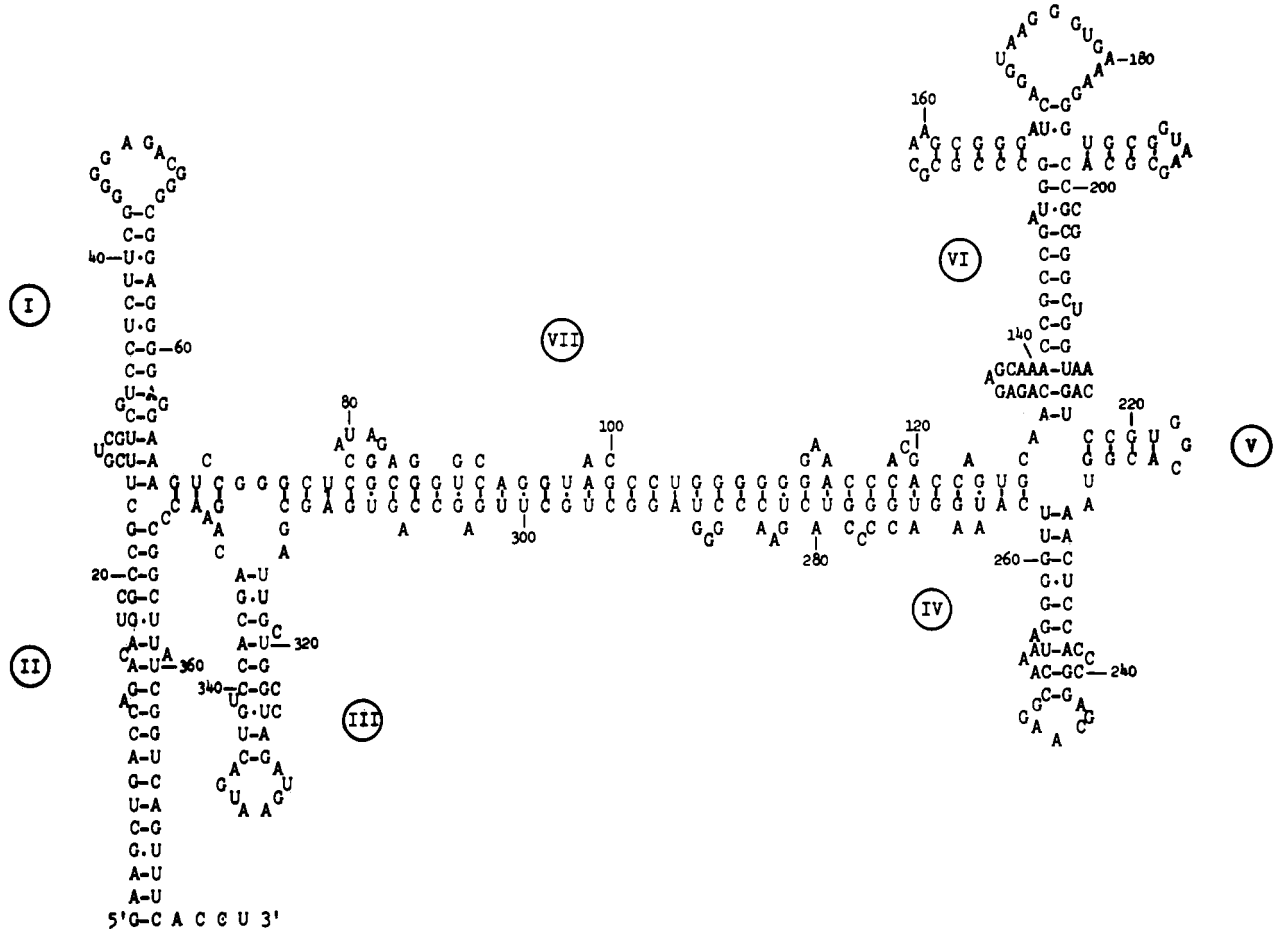

FIGURE 3: Original hypothetical model of the secondary structure of M1 RNA deduced from the nucleotide sequence of the gene encoding M1 RNA [Reed et al., 1982 (reprinted with permission)]. This model is missing the dinucleotide sequence AG which should be inserted after nucleotide 194. The two extra nucleotides do not alter the structure shown in any significant way.

function of M1 RNA. Similarly, preliminary data regarding the function of M1 RNA molecules lacking about 100 nucleotides proximal to the 3′ terminus indicate that both pentanucleotides cited above may be unnecessary for M1 RNA catalysis (unpublished experiments). None of the other structural features of the model shown in Figure 2 suggest any further insight into the catalytic mechanisms of cleavage by M1 RNA although additional data concerning nuclease susceptibility of M1 RNA in its "active" state (see below) may be useful in this regard.

Decisions regarding the single- or double-stranded nature of some regions of M1 RNA are not unambiguous. For example, most of the nucleotides from positions 227–236 appear to be susceptible to digestion by both nuclease S_1 and cobra venom nuclease. This result may reflect real differences in the structure observed in the buffers used for each nuclease (recall that nuclease S_1 requires Zn^{2+} for activity whereas digestions with cobra venom nuclease are carried out in buffers containing Mg^{2+}; see Materials and Methods) and the relatively small free energy of stabilization of the structures involving nucleotides 220–230 ($\Delta F \sim -4$ kcal) and 233–265 ($\Delta F \sim -7$ kcal). Free energies were calculated according to Gralla & Crothers (1973a,b) and Tinoco et al. (1973). In other regions which are shown as hydrogen bonded in the model, most notably nucleotides 74–78 and 342–345, one strand of a stem region is susceptible to S_1 nuclease and/or RNase A attack, but the other is sensitive to cobra venom nuclease. We cannot choose between two alternatives to explain the results: (a) these regions of supposed secondary structure have marginal thermodynamic stability and are not base paired a significant fraction of the time; (b) the hypothetical structure is incorrect, and these sequences should not at all be shown as being involved in base-paired structures.

The original model for the structure of M1 RNA (Figure 3) had six stem–loop structures and a long base-paired region joining domains III and IV. Regions II, III, IV, and V are virtually unchanged in our new model. The relative locations of loops I and VI are also unchanged, but the exact configuration of the sequences in the stems and loops has been somewhat modified. [All of the stem–loop structures shown in Figure 2 are stable according to the rules of Tinoco et al. (1973).] By contrast, our data indicate that the region connecting the left- and right-hand portions of the molecule (as shown in Figure 2) is much more complex than originally anticipated and contains several large internal loops, bulges, and connecting base-paired regions. In retrospect, it is apparent that domains having between 4 and 6 base pairs of marginal stability (for example, domains that contain G-U pairs and bulged-out nucleotides such as the hypothetical structures that involve nucleotides 85–95 interacting with 300–310, and nucleotides 110–120 with 275–285 as shown in Figure 3) should be left as unpaired regions rather than incorporated as internal paired segments with adjacent more stable regions.

In some regions of M1 RNA, there are insufficient data on sensitivity to nuclease digestion to distinguish between two or three possible stem–loop structures. For example, the nucleotides in regions 69–106 and 233–265 can be rearranged to translate the mismatched, bulged nucleotides from one part of the stem to another. While these details may ultimately be critical for determination of the unique structure–function relationships of M1 RNA, they do not significantly alter the

model at our current level of resolution.

As indicated above, some cleavages by RNases T_1 and A occur in double-stranded regions near G-U pairs or near bulged- or looped-out nucleotides. These cleavages may reflect "breathing" of double-stranded structures in these areas of secondary sites of cleavage which are readily exposed once a nearby cleavage has been made. Another striking aspect of the cleavage data is the absence of susceptibility to cobra venom of nucleotides 31–48 while the paired nucleotides 51–60 are all sensitive. In this stem structure, one strand consists entirely of pyrimidines and the other purines. In such structures, which probably do not have the standard A helical conformation, cobra venom nuclease may be exhibiting extreme specificity for the strand that contains exclusively purines. We note also that other regions sensitive to cobra venom nuclease but not involved in obvious base pairing may be important for tertiary interactions. In addition to nucleotides 174–176, 375–377, and 282–284 mentioned above, another such region is at nucleotides 22–24.

Active and Inactive States of M1 RNA. M1 RNA can catalyze the cleavage of tRNA precursor molecules in buffers containing 60 mM $MgCl_2$, in buffers containing 10 mM $MgCl_2$ plus 5 mM spermidine, or in buffers containing 10 mM $MgCl_2$ when the RNA is reconstituted with C5 protein to make the RNase P complex. In buffers containing 10 mM $MgCl_2$ with no added protein or polyamine, no catalytic activity of M1 RNA is observed (Guerrier-Takada et al., 1983). These and other observations indicate that M1 RNA may exist in either an active or an inactive species, depending on the concentration of Mg ions and the presence of other factors in solution. Accordingly, we initiated a comparative study of nuclease susceptibility patterns of M1 RNA under these different conditions. RNase T_1, which yields reproducible patterns and is active at both low and high Mg concentrations, was used in the experiments reported below.

The general features of M1 RNA structure, as reflected by susceptibility to mild digestion with RNase T_1, are the same in both the inactive and active forms. For example, the pattern shown in lane 8 of Figure 4 is a result of a digest performed in buffer containing 10 mM $MgCl_2$ (inactive form) whereas the patterns shown in lane 4 of figure 4 (digest performed in buffer containing 60 mM $MgCl_2$) and lane 7 of Figure 4 (digest performed in buffer containing 10 mM $MgCl_2$ on M1 RNA reconstituted with C5 protein) reflect the pattern found in the active form. In all cases, the major products of digestion are identical (note, for example, the preservation of major cleavage sites at nucleotides 276, 296, and 310). However, some differences in the patterns are apparent in their details and are indicative of structural differences between the inactive and active forms. Note that the G residues at positions 270, 285, and 336 are more susceptible to RNase T_1 attack in the inactive conformation (lane 8) than in the active forms (lanes 4 and 7). These data indicate that the active conformation of M1 RNA is the same, whether achieved in the presence of a high Mg^{2+} concentration or by reconstitution with C5 protein at low Mg^{2+} concentration.

We have probed the structure of M1 RNA in the presence of a substrate molecule, the precursor to $tRNA^{Tyr}$, from *E. coli*[2] to determine if the structure is changed by virtue of interaction with the substrate. As shown in lanes 2 and 5 of Figure 4, the structure of uniformly labeled pTyr appears identical in buffers that contain either 10 or 60 mM $MgCl_2$. Lanes 3 and 6 are digestion patterns of either the binary complex of M1 RNA and pTyr in 60 mM $MgCl_2$ or the ternary complex of M1 RNA, C5 protein, and pTyr in buffer

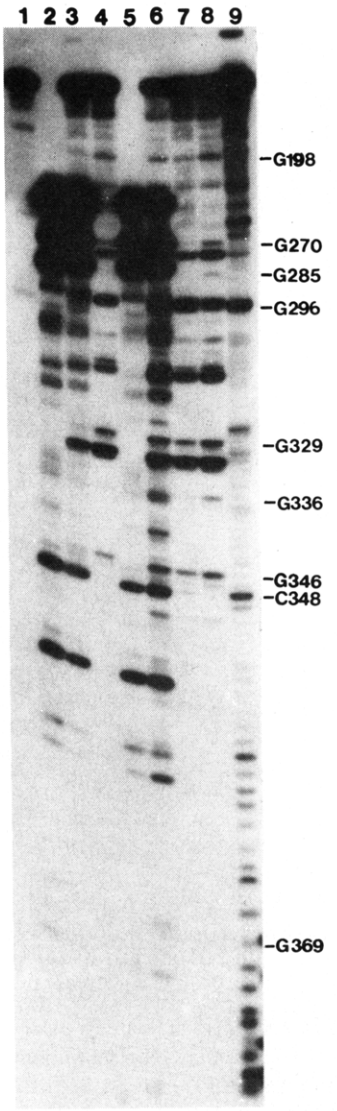

FIGURE 4: Results of mild digestion of M1 RNA with RNase T_1. M1 RNA (6×10^3 cpm) was digested at 0 °C for 1 min in the absence or presence of C5 protein (the protein subunit of *E. coli* RNase P) and/or ^{32}P-labeled precursor to *E. coli* $tRNA^{Tyr}$ (1×10^4 cpm; abbreviated as pTyr). The M1 RNA used was labeled at its 3′ terminus. The experiments shown in lanes 3 and 6 involve partial digests by RNase T_1 of two different labeled RNA molecules. The sensitivity of particular sites to RNase T_1 digestion is mentioned in the text only when such sites can be unequivocally assigned to either M1 RNA or pTyr by comparison with digests of either molecule alone as shown in lanes 2, 4, 5, and 7. Lane 1, M1 RNA with *no* RNase T_1 added (buffer C: 50 mM Tris-HCl, pH 7.6, 100 mM NH_4Cl, 60 mM $MgCl_2$, and 5% glycerol); lane 2, pTyr in buffer C; lane 3, pTyr plus M1 RNA in buffer C; lane 4, M1 RNA (buffer C); lane 5, pTyr in buffer B (50 mM Tris-HCl, pH 7.6, 60 mM NH_4Cl, and 10 mM $MgCl_2$); lane 6, reconstituted *E. coli* RNase P (C5 protein + M1 RNA) plus pTyr in buffer B; lane 7, reconstituted *E. coli* RNase P (C5 protein + M1 RNA) plus pTyr in buffer B; lane 7, reconstituted *E. coli* RNase P (C5 protein + M1 RNA) in buffer B; lane 8, M1 RNA (buffer B); lane 9, M1 RNA (mild alkaline digest) with *no* RNase T_1 added.

that contains 10 mM $MgCl_2$. Even though both RNA molecules are labeled with ^{32}P, careful analysis of the digest patterns allows us to identify sites specific to M1 RNA or pTyr (see legend to Figure 4). We note that the pattern shown in lane 3 indicates that G residues at positions 310, 329, and 346 in M1 RNA are less susceptible to nuclease digestion in the binary complex than when M1 RNA is alone in solution (lane 4) *or* when it is present in the ternary complex (lane 6). In this respect, it appears that the structure of M1 RNA during

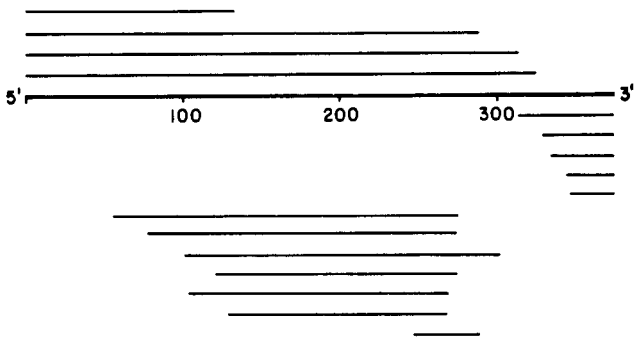

FIGURE 5: Diagram indicating RNase T_1 cleavage sites on uniformly labeled M1 RNA. The fragments produced by mild digestion with the nuclease were identified by their RNase T_1 fingerprint pattern. The end points of the fragments are shown in the sketch as a distance along the abscissa measured in nucleotides.

its interaction with pTyr may change depending on whether or not C5 is part of the RNase P complex. These observations must be confirmed by experiments with other nucleases. Note also that at least two residues in pTyr (Figure 4, lane 3) are also protected in the binary complex.

We have observed in separate experiments that bases G329 and G336 in M1 RNA become more accessible if M1 RNA is incubated in steps from 37 to 58 °C prior to nuclease treatments and that this phenomenon is directly correlated with a drop in catalytic activity of M1 RNA as the temperature of incubation is raised. In the absence of more data, however, we cannot draw a more coherent picture of how the structural transition is achieved between the two conformations of M1 RNA.

Although the experiment shown in lane 7 of Figure 4 indicates that there is a moderate protection of all cleavage sites between nucleotides 100 and 285 of M1 RNA, we do not regard this as a definitive footprint since the relative concentration of C5 may have been too low to provide stoichiometric protection of a region in M1 RNA. We do note, however, that in the presence of C5 protein the "active form" of M1 RNA seems to be hydrolyzed at C343, C348, and C367 (Figure 4, lane 7) although this effect is not seen with all preparations of the protein. We previously observed that the products of radioautolysis of M1 RNA appeared to be enhanced in the presence of C5 protein, perhaps because the protein imposed additional strain on specific bonds in the phosphodiester backbone of the RNA. Whether this can be considered as evidence for nuclease activity associated with C5 protein, we cannot yet say. A more detailed study of interactions between C5 protein and M1 RNA will be reported elsewhere.

Experiments with Uniformly Labeled M1 RNA. We have also performed partial digests with RNase T_1 of M1 RNA molecules that have been uniformly labeled in vivo to see if the cleavage sites observed would be in agreement with those observed with RNA molecules that have been end labeled in vitro and to generate M1 RNA fragments for use in tests of catalytic function. RNase T_1 digests were performed as described (Reed et al., 1982), and RNA fragments were resolved on a 5% denaturing gel. After electroelution of RNA from gel slices, a complete RNase T_1 fingerprint pattern of each fragment was obtained (data not shown). The end points of some fragments could be unequivocally identified from the fingerprints, and these are indicated in Figure 5. As expected, most of the cleavage sites are located in single-stranded regions. The exceptions are at residues G55, G290, and G291 (or G292) which are, however, located adjacent to bulges in the helix structure. Cleavage at these sites can be explained as secondary RNase T_1 cleavage sites occurring after the unfolding of the molecule that follows the cleavage at a primary site. (One can infer from these and earlier results that 3′ end labeling of M1 RNA molecules using pCp and RNA ligase did not alter the secondary structure of the molecule. End-labeled M1 RNA can, therefore, be used for further studies involving binding to C5 protein.)

Discussion

The secondary structure of M1 RNA in solution has been probed with various nucleases specific for either single- or double-stranded regions of RNA. From these data, we have generated a model for the secondary structure of M1 RNA which is similar to one previously constructed from purely theoretical considerations. Certain sites in M1 RNA are attacked by the double-stranded-specific cobra venom nuclease but appear in single-stranded regions in our model. The particular nucleotide sequences involved are compatible with the idea that these sites participate in tertiary structural interactions and govern folding of M1 RNA. Further work is required to verify this hypothesis. Similarly, the nucleases specific for single-stranded regions attack some sites that are shown in our model as double-stranded regions. These cleavages may be "secondary" cleavages of M1 RNA or may be located in regions which are marginally unstable in a "local sense" (i.e., adjacent to G-U pairs or near the junction between single- and double-stranded regions). On the other hand, discrepancies between empirical data and model building may be due to incorrect features of the model and our inability to make all the data fit a particular model. Nevertheless, the current model of M1 RNA has some features which are unaffected by these discrepancies and which enable us to test specific ideas of M1 RNA function and to probe further the structure of M1 RNA with additional chemical and enzymatic agents.

By all the criteria tested, it appears that nucleotides 330–336 are available for hydrogen-bonding interactions with the complementary sequence (GTΨCPu) which exists in all tRNA precursor substrates. Another region of complementarity to the TΨC loop of tRNA precursors is found at nucleotides 284–288, but this sequence, although shown in a small loop region, is not as accessible to nuclease attack and presumably, therefore, not easily available for hydrogen-bonding interactions. Site-directed mutagenesis experiments, now under way, will elucidate the role of these regions in substrate recognition.

Structures for M1 RNA generated by computer programs that we based on purely theoretical base-pairing possibilities are quite different from the structure portrayed in Figure 2 unless additional constraints are added. These constraints are (a) that the 5′ and 3′ terminal sequences of M1 RNA should be base paired and (b) that the data regarding nuclease-sensitive sites should be incorporated as much as possible into the model building. Even with the added constraints, computer-generated structures have more discrepancies with respect to the nuclease sensitivity data than the structure shown in Figure 2. Nevertheless, the best structures drawn by either method have many features in common. In the absence of further data regarding tertiary interactions, it is of marginal utility to explore the variations in secondary structure which are generated by various computer models.

Our previous studies of the enzymatic function of M1 RNA indicated that this molecule exists in either an active or an inactive conformation, depending on the buffer composition and/or prior physical treatment. Data from the nuclease digestion experiments show that there are two conformers of M1 RNA which are sensitive to the concentration of Mg ions

and the presence or absence of C5 protein but that these conformers share most features of the secondary structure of the molecule. (We do not have insight yet into the tertiary conformation of M1 RNA in either state.) The subtle changes observed in the secondary structure of M1 RNA in the two forms may reflect functional properties which we have yet to identify. In addition, the pTyr substrate also changes somewhat in its conformation when in the binary complex with M1 RNA.

Our experiments provide the first empirical description of the secondary structure of a true RNA enzyme. The structure is complex and as yet incompletely determined, especially with respect to its three-dimensional characteristics. Another RNA which may have catalytic properties, the intervening sequence of a *Tetrahymena* rRNA precursor molecule, has also been described at the same level of analysis (Cech et al., 1983). Both molecules are replete with stem–loop structures, as are most biologically important RNA molecules, but do not show any marked homologies to each other in sequence or structure. The features of each which bear some resemblance are hydrogen-bonded structures of more than seven nucleotides which consist of strands which are all pyrimidines or all purines, and a very long stem structure extremely rich in G-C and G-U pairs. Whether or not these rough features of stem–loop structures are important for catalysis cannot be determined at present.

Acknowledgments

We thank our colleagues for stimulating discussions and Dr. Ann Korner for help with the manuscript.

Registry No. RNase P, 71427-00-4.

References

Altman, S., Bowman, E. J., Garber, R. L., Kole, R., Koski, R. A., & Stark, B. C. (1980) *tRNA: Biological Aspects* (Abelson, J., Schimmel, P., & Soll, D., Eds) pp 71–82, Cold Spring Harbor Laboratory, Cold Spring Harbor, NY.

Avron, P. E., Weber, L. D., & Rich, A. (1982) *Biochemistry 21*, 4700–4706.

Cech, T. R., Tanner, N. K., Tinoco, I., Jr., Weir, B. R., Zuker, M., & Perlman, P. S. (1983) *Proc. Natl. Acad. Sci. U.S.A. 80*, 3903–3907.

Donis-Keller, H., Maxam, A., & Gilbert, W. (1977) *Nucleic Acids Res. 4*, 2527–2538.

England, T. E., Bruce, A. G., & Uhlenbeck, O. C. (1980) *Methods Enzymol. 65*, 65–75.

Garrett, R. A., & Olesen, S. O. (1982) *Biochemistry 21*, 4823–4830.

Gralla, J., & Crothers, D. M. (1973a) *J. Mol. Biol. 73*, 497–511.

Gralla, J., & Crothers, D. M. (1973b) *J. Mol. Biol. 78*, 301–319.

Guerrier-Takada, C., & Altman, S. (1984) *Science (Washington, D.C.) 223*, 285–286.

Guerrier-Takada, C., Gardiner, K., Marsh, T., Pace, N., & Altman, S. (1983) *Cell (Cambridge, Mass.) 35*, 849–857.

Maniatis, T., Fritsch, E. F., & Sambrook, J. (1982) *Molecular cloning (A Laboratory Manual)* pp 458–459, Cold Spring Harbor Laboratory, Cold Spring Harbor, NY.

Platt, T., & Yanofsky, C. (1975) *Proc. Natl. Acad. Sci. U.S.A. 72*, 2399–2403.

Reed, R. E., Baer, M. F., Guerrier-Takada, C., Donis-Keller, H., & Altman, S. (1982) *Cell (Cambridge, Mass.) 30*, 627–636.

Sakamoto, H., Kimura, N., Nagawa, F., & Shimura, Y. (1983) *Nucleic Acids Res. 11*, 8237–8251.

Tinoco, I., Borer, P. N., Dingler, B., Levine, M. D., Uhlenbeck, O. C., Crothers, D. M., & Gralla, J. (1973) *Nature (London), New Biol. 246*, 40–41.

Wurst, R. M., Vournakis, J. N., & Maxam, A. M. (1978) *Biochemistry 17*, 4493–4499.

Vasilenko, S. K., Butorin, A. S., Maev, S. P., Vityugov, F. I., Boldyreva, L. G., & Rait, V. K. (1983) *Mol. Biol. (Engl. Transl.) 17*, 818–826.